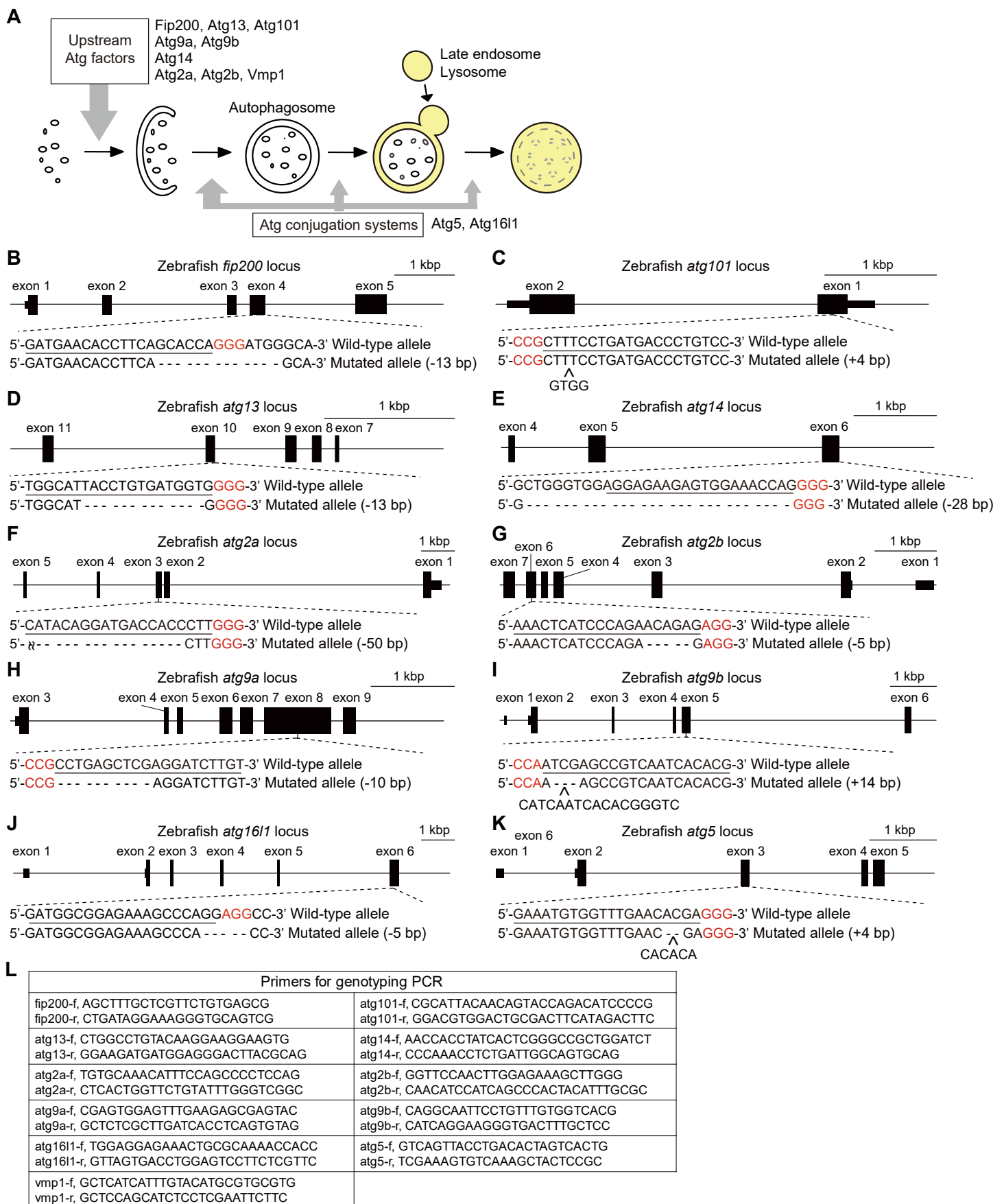


**Supplemental Information**

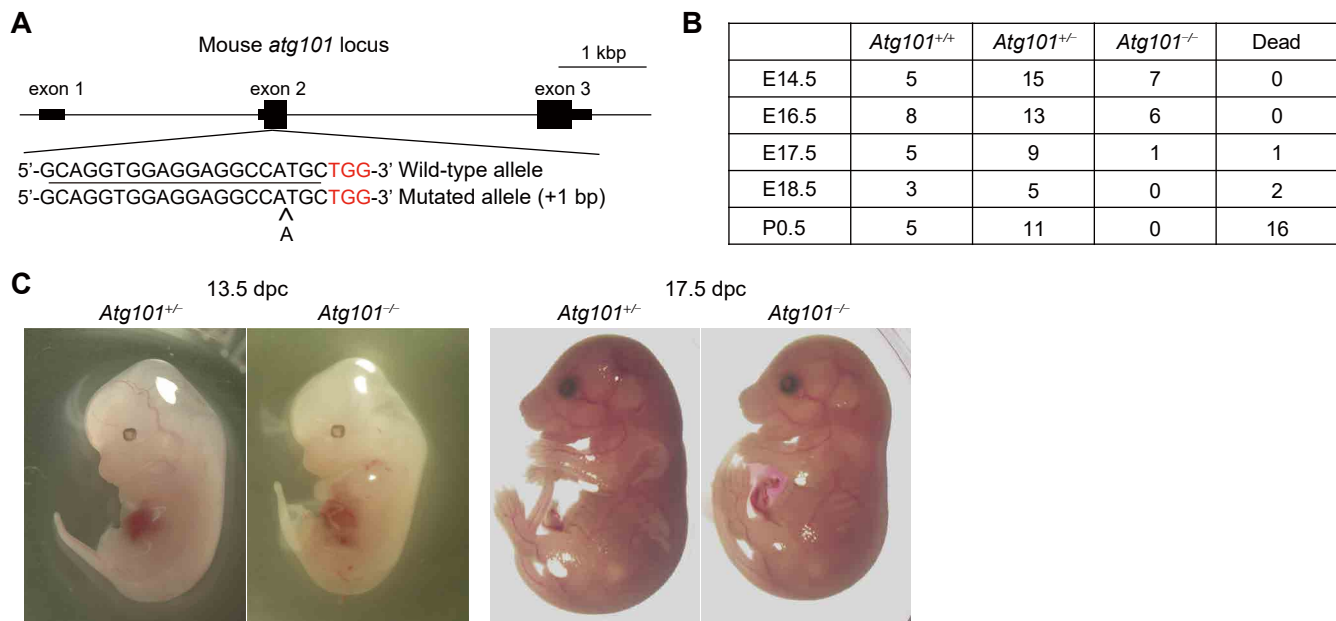
**Autophagy Is Required for Maturation  
of Surfactant-Containing Lamellar Bodies  
in the Lung and Swim Bladder**

**Hideaki Morishita, Yuki Kanda, Takeshi Kaizuka, Haruka Chino, Kazuki Nakao, Yoshimi Miki, Yoshitaka Takeuchi, Jun-Lin Guan, Makoto Murakami, Atsu Aiba, and Noboru Mizushima**



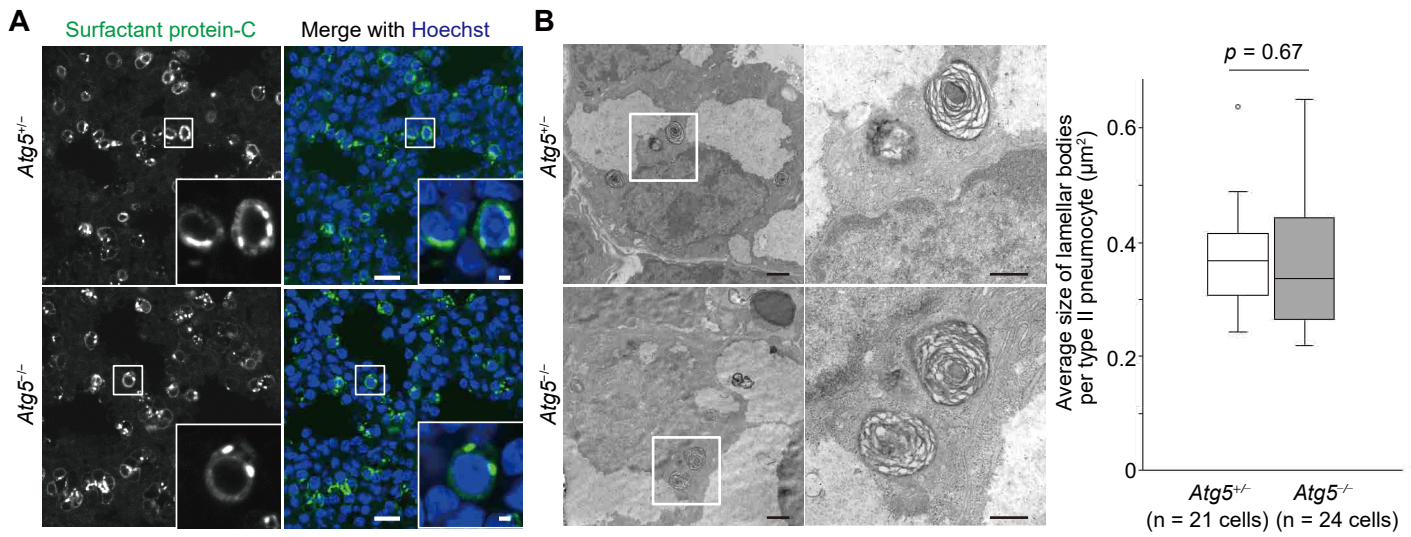
**Figure S1 Generation of *atg*-deficient zebrafish using CRISPR/Cas9 system, Related to Figure 1**

(A) A schematic model of the functional steps of Atg proteins during autophagy in vertebrates.  
 (B–L) Schematic representation of the Cas9-gRNA-targeted sites in the zebrafish loci for *fip200* (B), *atg101* (C), *atg13* (D), *atg14* (E), *atg2a* (F), *atg2b* (G), *atg9a* (H), *atg9b* (I), *atg16l1* (J), and *atg5* (K). The protospacer-adjacent motif (PAM) sequence is shown in red. The targeted sites are underlined. Sequences for wild-type and mutated alleles are shown. Primers for genotyping PCR of each line are shown (L).



**Figure S2 Generation of *Atg101*-deficient mice, Related to Figure 4**

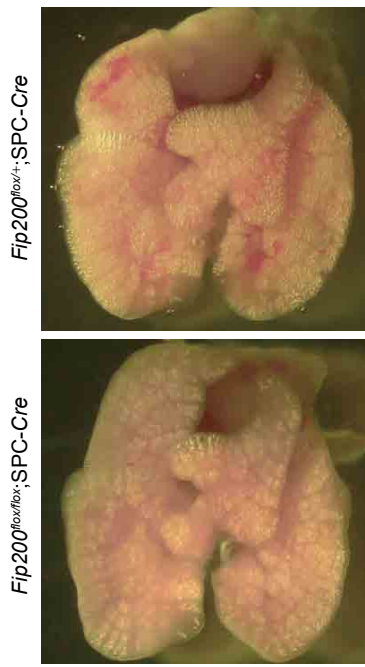
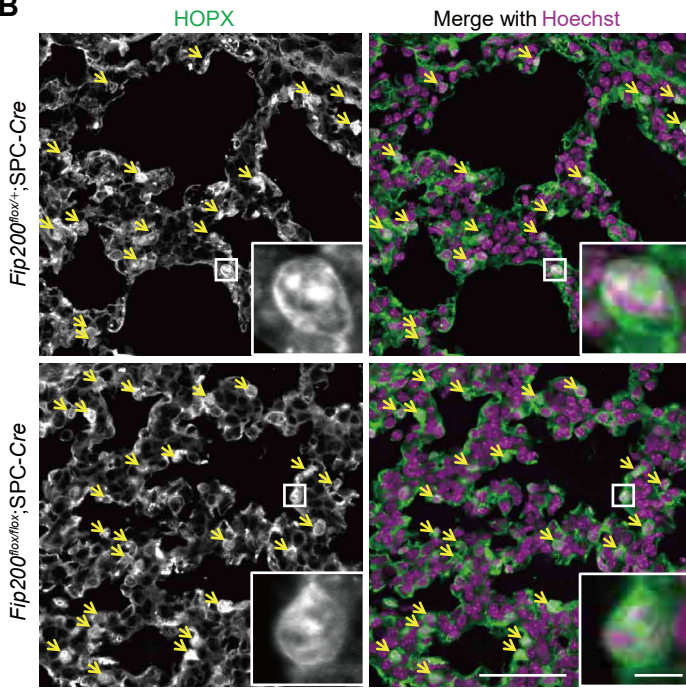
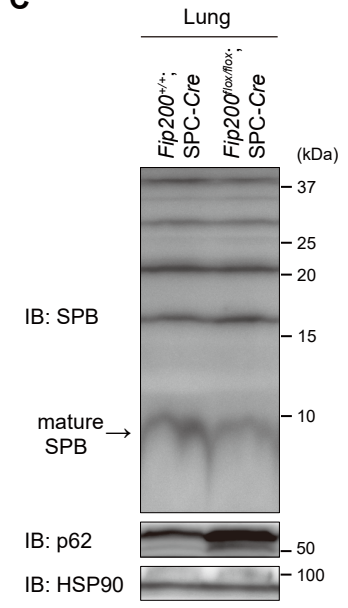
(A) Schematic representation of the Cas9-gRNA-targeted site in the mouse *Atg101* locus. The PAM sequence is shown in red. The targeted site is underlined. Sequences for wild-type and mutated alleles are shown.  
 (B) Survival rate of offspring from intercrosses of *Atg101*<sup>+/-</sup> mice.  
 (C) External appearance of *Atg101*<sup>+/-</sup> and *Atg101*<sup>-/-</sup> mice at 13.5 dpc and 17.5 dpc.



**Figure S3 ATG5 is dispensable for maturation of lamellar bodies in type II pneumocytes in mice, Related to Figure 4**

(A) Immunohistochemistry of lungs from 17.5-dpc *Atg5<sup>+/−</sup>* and *Atg5<sup>−/−</sup>* mice using anti-SPC antibody. Nuclear DNA was stained with Hoechst33342. Scale bar, 20  $\mu\text{m}$  and 2  $\mu\text{m}$  in the inset.

(B) Transmission electron microscopy of type II pneumocytes from 17.5-dpc *Atg5<sup>+/−</sup>* and *Atg5<sup>−/−</sup>* mice. Magnified images of the indicated regions are shown in the right panels. The average size (cross sectional area) of each lamellar body was quantified (21 cells and 24 cells for *Atg5<sup>+/−</sup>* and *Atg5<sup>−/−</sup>* mice, respectively). The solid bars and boxes indicate the median and interquartile range (25th to 75th percentile), respectively. The whiskers indicate the upper and lower quartiles, and outliers are plotted individually. Scale bar, 1  $\mu\text{m}$  and 400 nm in magnified panels. An unpaired two-tailed Mann-Whitney's U test was used to compare the two groups.

**A****B****C**

**Figure S4 Deletion of *Fip200* in type II pneumocytes did not disrupt lung morphogenesis and type I pneumocyte differentiation in mice, Related to Figure 4**

(A) External appearance of the lung of neonatal *Fip200<sup>+/+</sup>;SPC-Cre* and *Fip200<sup>fl/fl</sup>;SPC-Cre* mice at 1 hour after birth. (B) Immunohistochemistry of the lung of neonatal *Fip200<sup>+/+</sup>;SPC-Cre* and *Fip200<sup>fl/fl</sup>;SPC-Cre* mice at 1 hour after birth using anti-HOPX (a marker for type I pneumocytes) antibody. Nuclear DNA was stained with Hoechst33342. Scale bar, 50 µm and 5 µm in the insets. Arrows indicate nuclear staining of HOPX. Data are representative of at least two mice of each genotype.

(C) Immunoblotting of SPB, p62, and HSP90 in the lung of *Fip200<sup>+/+</sup>;SPC-Cre* and *Fip200<sup>fl/fl</sup>;SPC-Cre* mice at 1 hour after birth. An arrow indicates the mature form of SPB.